Extraordinary Magnetic Field Enhancement with Metallic Nanowire: Role of Surface Impedance in Babinet's Principle for Sub-Skin-Depth Regime

Sukmo Koo,[1] M. Sathish Kumar,[1] Jonghwa Shin,[2] DaiSik Kim,[3] and Namkyoo Park[1,*]

[1]*Photonic Systems Laboratory, School of EECS, Seoul National University, Seoul 151-744, Korea*

[2]*Department of Physics, Korea Advanced Institute of Science and Technology, Daejeon 305-701, Korea*

[3]*Center for Subwavelength Optics, Department of Physics and Astronomy, Seoul National University, Seoul 151-747, Korea*

(Received 17 July 2009; published 21 December 2009)

We propose and analyze the "complementary" structure of a metallic nanogap, namely, the metallic nanowire for magnetic field enhancement. A huge enhancement of the field up to a factor of 300 was achieved. Introducing the surface impedance concept, we also develop and numerically confirm a new analytic theory which successfully predicts the field enhancement factors for metal nanostructures. Compared to the predictions of the classical Babinet principle applied to a nanogap, an order of magnitude difference in the field enhancement factor was observed for the sub-skin-depth regime nanowire.

DOI: 10.1103/PhysRevLett.103.263901 PACS numbers: 42.25.Bs, 41.20.Jb, 42.79.Ag, 78.66.Bz

It is well known that nanosized metallic structures such as nanogaps can achieve huge electric field enhancement through the phenomena of extraordinary transmission (EOT) [1–11]. Recent developments in EOT include the demonstration of nonresonant, factor of 1000 enhancements in the electric field, through a $\lambda/30\,000$ slit on metal films and thereby extending the concept of extraordinary transmission deep into the sub-skin-depth regime [11]. Considering the increasing attention towards magnetic field enhancement with its potential applications, such as in magnetic nonlinearity and devices based thereon [12], achieving magnetic field enhancement is as important an issue in nanophotonics as achieving electric field enhancement. Though a simple approach to achieve this goal can be found in the well-known Babinet principle [13], considering the nonideal nature of real metal, an in-depth investigation of Babinet's principle is warranted. As an example, the partial disagreement of experimental results with the predictions of Babinet's principle in [14] has been attributed to the nonideal nature of real metals and possibly fabrication error in the sample.

In this Letter, motivated by Babinet's principle, we propose the metallic nanowire (complementary of nanogap in [11], which could be fabricated, for example, by using the method in [15]) to achieve extraordinary magnetic field enhancement by a factor of 300. Further, for the first time to the best of our knowledge, we also develop a comprehensive theory to explain the difference in field enhancement between the electric and magnetic fields in complementary metallic nanostructures, and to correctly predict the enhancement of magnetic field in the sub-skin-depth regime. In sharp contrast to the predictions of the classical Babinet's principle applied to the result of [11]—where the enhancement factor of electric field scaled only with the inverse of gap width, our analysis shows that the magnetic field enhancement of nanowire has strong dependence on the fundamental scaling length—metal skin depth. Orders of difference in the field enhancement were observed between nanogap and nanowire. Results show excellent agreement of the developed theory with the finite-difference time-domain (FDTD) analysis.

Figure 1 shows the system under consideration. Figure 1(a) is the nanogap and Fig. 1(b) is the nanowire. A plane wave of wavelength λ_0 impinges normally on these structures. The polarization considered is transverse magnetic (TM) for the nanogap and transverse electric (TE) for the nanowire. For the present, the thickness of the structure is assumed to be infinitesimal so as to isolate the effect of nonzero impedance of the real metal on the complementary scattering behavior. The effects of finite thickness on the scattering are discussed later. R_s stands for the surface resistivity in ohms per square. When $R_s = 0$, the metal becomes a perfect electric conductor (PEC).

The field H_z (E_z) for the TM (TE) wave in free space for 2D problems can be expressed as below:

$$\frac{\partial^2 H_z(E_z)}{\partial x^2} + \frac{\partial^2 H_z(E_z)}{\partial y^2} + k_0{}^2 H_z(E_z) = 0. \qquad (1)$$

A general solution of (1) can be expressed as a linear combination of plane waves. With the scattering objects

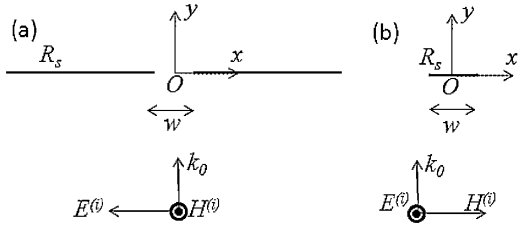

FIG. 1. Diagram of the (a) nanogap and (b) nanowire structure having width w and infinitesimal thickness. R_s is the surface resistivity of the metal in ohms per square, and Z is the free space impedance. The structure is illuminated by the TM (TE) wave for the nanogap (nanowire) having wavelength $\lambda_0 = 2\pi/k_0$. The superscript (i) denotes incident fields.

at $y = 0$, following the procedures in [13], the scattered field components can be shown to be as

$$H_z^{(s)} = \pm \int_C P(\cos\alpha)\exp[ik_0 r\cos(\theta \mp \alpha)]d\alpha \qquad E_x^{(s)} = -Z\int_C \sin\alpha P(\cos\alpha)\exp[ik_0 r\cos(\theta \mp \alpha)]d\alpha$$
$$E_y^{(s)} = \pm Z\int_C \cos\alpha P(\cos\alpha)\exp[ik_0 r\cos(\theta \mp \alpha)]d\alpha, \tag{2}$$

$$E_z^{(s)} = \int_C P(\cos\alpha)\exp[ik_0 r\cos(\theta \mp \alpha)]d\alpha \qquad H_x^{(s)} = \pm\frac{1}{Z}\int_C \sin\alpha P(\cos\alpha)\exp[ik_0 r\cos(\theta \mp \alpha)]d\alpha$$
$$H_y^{(s)} = -\frac{1}{Z}\int_C \cos\alpha P(\cos\alpha)\exp[ik_0 r\cos(\theta \mp \alpha)]d\alpha, \tag{3}$$

respectively, for TM and TE incidence. Here k_0 and Z are the wave number and impedance, respectively, in free space. C is the path in the complex α plane along which $\cos\alpha$ ranges through real values from $-\infty$ to ∞ [13]. The superscript (s) denotes scattered components ($\boldsymbol{E} = \boldsymbol{E}^{(i)} + \boldsymbol{E}^{(s)}$, $\boldsymbol{H} = \boldsymbol{H}^{(i)} + \boldsymbol{H}^{(s)}$) and the upper sign is for $y > 0$ and the lower sign is for $y < 0$.

The boundary conditions for infinitesimally thin metals are well known [16] and so are the symmetry conditions on the scattered fields [13], as given below:

$$\begin{pmatrix} \hat{\mathbf{n}} \times [\mathbf{E}(y = 0+) - \mathbf{E}(y = 0-)] = 0 & \text{on air} \\ R_s\mathbf{J_s} = R_s\{\hat{\mathbf{n}} \times [\mathbf{H}(y = 0+) - \mathbf{H}(y = 0-)]\} = -\hat{\mathbf{n}} \times \hat{\mathbf{n}} \times \mathbf{E}(y = 0) & \text{on metal} \end{pmatrix}, \tag{4}$$

$$\begin{pmatrix} H_x^{(s)}(y = 0+) = -H_x^{(s)}(y = 0-) \\ H_y^{(s)}(y = 0+) = H_y^{(s)}(y = 0-) \\ H_z^{(s)}(y = 0+) = -H_z^{(s)}(y = 0-) \end{pmatrix} \qquad \begin{pmatrix} E_x^{(s)}(y = 0+) = E_x^{(s)}(y = 0-) \\ E_y^{(s)}(y = 0+) = -E_y^{(s)}(y = 0-) \\ E_z^{(s)}(y = 0+) = E_z^{(s)}(y = 0-) \end{pmatrix}. \tag{5}$$

Here $\boldsymbol{n}$ is the outward unit vector parallel to the $+y$ direction and $\boldsymbol{J_s}$ is the surface current density. Now putting (2) and (3) into (4) and (5) we can arrive at the dual integral equations to be solved for $P(\cos\alpha)$. At $y = 0+$, with $\cos\alpha = \mu$, for nanogap (6) and nanowire (7) we get

$$\int_{-\infty}^{\infty}\frac{P(\mu)}{\sqrt{1-\mu^2}}\exp(ik_0 x\mu)d\mu = 0 \text{ for}\left(|x| < \frac{w}{2}\right), \quad \int_{-\infty}^{\infty}\left(\frac{2R_s}{\sqrt{1-\mu^2}} + Z\right)P(\mu)\exp(ik_0 x\mu)d\mu = E^{(i)} \text{ for}\left(|x| > \frac{w}{2}\right), \tag{6}$$

$$\int_{-\infty}^{\infty}\left(\frac{1}{\sqrt{1-\mu^2}} + 2\frac{R_s}{Z}\right)P(\mu)\exp(ik_0 x\mu)d\mu = -ZH^{(i)} \text{ for}\left(|x| < \frac{w}{2}\right), \quad \int_{-\infty}^{\infty}P(\mu)\exp(ik_0 x\mu)d\mu = 0 \text{ for}\left(|x| > \frac{w}{2}\right). \tag{7}$$

Using the convolution theorem [17] from spectral analysis, we can express (6) and (7) as, for nanogap (8) and nanowire (9)

$$\int_{-\infty}^{\infty}E_x^{(s)}(x')c(x - x')dx' = 0 \text{ for}\left(|x| < \frac{w}{2}\right), \quad -\frac{k_0 R_s}{Z\pi}\int_{-\infty}^{\infty}E_x^{(s)}(x')c(x - x')dx' - E_x^{(s)}(x) = E^{(i)} \text{ for}\left(|x| > \frac{w}{2}\right), \tag{8}$$

$$\frac{k_0}{2\pi}\int_{-\infty}^{\infty}H_x^{(s)}(x')c(x - x')dx' + 2\frac{R_s}{Z}H_x^{(s)}(x) = -H^{(i)} \text{ for}\left(|x| < \frac{w}{2}\right), \qquad H_x^{(s)}(x) = 0 \text{ for}\left(|x| > \frac{w}{2}\right), \tag{9}$$

where

$$c(x) = \int_{-\infty}^{\infty}\frac{1}{\sqrt{1-\mu^2}}\exp(ik_0 x\mu)d\mu = \pi[J_0(k_0 x) + iY_0(|k_0 x|)]$$

and w is the width of the nanogap or nanowire (Fig. 1). Here $J_0(x)$ and $Y_0(x)$ are Bessel functions of the first and second kinds of order zero, respectively. Considering that $k_0 w$ will be very small, the Bessel functions can be approximated in terms of $k_0 w$ and $\ln(k_0 w)$. Further, using the average field values, $E_{x0}(R_s)$ (gap) and $H_{x0}(R_s)$ (wire) for the range $|x| < w/2$ in (8) and (9), respectively, we get expressions for electric [magnetic] field strengths for PEC ($R_s = 0$) as

$$E_{x0}(R_s = 0)[H_{x0}(R_s = 0)] \cong \frac{E^{(i)}[-H^{(i)}]}{k_0 w\{0.5 + \frac{i}{\pi}[\ln(k_0 w/4) - \gamma - 1]\}}. \tag{10}$$

For cases of real metal (nonzero R_s), we also obtain

$$\frac{E_{x0}(R_s)}{E^{(i)}} \cong \frac{E_{x0}(0)/E^{(i)}}{1 + 2R_s/Z}$$
$$\frac{H_{x0}(R_s)}{H^{(i)}} \cong \frac{H_{x0}(0)/H^{(i)}}{1 - 2(R_s/Z)H_{x0}(0)/H^{(i)}}, \tag{11}$$

where $\gamma(\approx 0.577)$ is the Euler constant. Equation (10) shows $\sim 1/f$ as well as $\sim 1/w$ dependence of the field enhancement in the nanogap which agrees perfectly with the earlier experimental and numerical results [11].

Equations (10) and (11) above show that the field enhancement in the nanogap and nanowire remains the same for both the cases if the metals are PECs ($R_s = 0$). To verify this, we simulated the nanowire and nanogap structures using FDTD. The simulation result assuming perfect conductor has been plotted in Figs. 2(a) and 2(b) for thickness that is small enough ($t = 40$ nm, $w = 1$ μm) so that the effect of finite thickness on field distribution is suppressed. To note, though the example considered here is from [11], our analysis applies equally well to other values of t and w as long as $w \ll \lambda$. An enhancement factor as high as ~ 1000 could be achieved both for electric field $[E_{x0}(0)/E^{(i)}]$ and magnetic field $[H_{x0}(0)/H^{(i)}]$ with dimensions $t = 4$ nm and $w = 145$ nm [Fig. 3(a)].

Now for the real metal, from (11) the behavior of field enhancement is quite different for the nanowire from that of the nanogap. For the nanogap, the field enhancement does not reduce as R_s increases (real metal) because the resistivity of the metal R_s is much smaller compared to Z in general. However, for the nanowire, the product R_s/Z in the denominator gets multiplied by $H_{x0}(0)/H^{(i)}$ causing reduction in magnetic field enhancement as R_s increases.

Equation (11) is not complete in the sense that the effects of finite thickness have been ignored. As the thickness increases, the conditions given in (4) and (5) are no longer valid. We name this as the geometric effect. This geometric effect can be accounted for in the analysis by assuming the current distribution to be essentially uniform within the wire, as long as t is smaller than the skin depth δ.

This small t assumption also means that we are in the negligible retardation regime and the induced current in the nanowire only depends on R_s and not on t by itself. Under this condition, for the same amount of flux impinging on wires of identical widths w, the current I will be constant given by $I = H_{x0}(R_s, t)(2w + 2t) = H_{x0}(R_s, 0)(2w)$. Now the expression for nanowire that takes into account the effect of finite thickness can be arrived at by multiplying Eq. (11) with $w/(w + t)$

$$\frac{H_{x0}(R_s, t)}{H^{(i)}} = \frac{[H_{x0}(0, 0)/H^{(i)}]w}{[1 - 2(R_s/Z)H_{x0}(0, 0)/H^{(i)}](w + t)}. \quad (12)$$

Arriving at the final equation for field enhancement including the geometric effect, we now study the field enhancement dependence on skin depth. Expressing field enhancement in terms of the skin depth (for the case of the nanowire) by writing $R_s = \rho/t$ [18] as $\delta^2\omega\mu_0/2t$ (holds for low frequency, when $t < \delta$) in Eq. (12) where ρ is the resistivity, we get

$$\frac{H_{x0}(R_s, t)}{H^{(i)}} = \frac{H_{x0}(0, 0)/H^{(i)}}{1 + (\delta^2/wt)\frac{\pi}{\{\pi/2 + i[\ln(k_0 w/4) - \gamma - 1]\}}} \frac{w}{w + t}$$
$$= \frac{H_{x0}(0, 0)/H^{(i)}}{1 + (\delta^2/wt)b} \frac{w}{w + t},$$
$$b = \frac{\pi}{\{\pi/2 + i[\ln(k_0 w/4) - \gamma - 1]\}}. \quad (13)$$

The term b above being of the order of 1, the magnetic field enhancement reduces when the product of (w/δ) and (t/δ) becomes smaller than 1. Figure 3 shows the magnetic field enhancement for different wire width and thickness. Perfect agreement is observed between calculated and numerically obtained results. For the electric field of nanogap, dependence on slit thickness was found to be negligible [Eq. (11) and FDTD data in Fig. 3(b)].

While the electric field enhancement of nanogap scales linearly with the reduction of gap width (even in the sub-skin-depth regime [11]), Eq. (13) and FDTD result in Fig. 3 above shows that the case is different for nanowire if w/δ or t/δ (dotted black lines in Fig. 3) is smaller than 1. Thus, contrary to the case of nanogap, an increase in the magnetic field enhancement of nanowire does not correlate well with the wire width but saturates in the sub-skin-depth regime, leading to a fundamental scaling length especially for magnetic field—the metal skin depth.

To put it intuitively, the outcome of the above analysis is that for the case of nanowire having finite conductivity, due to its boundary condition the magnetic field penetrates into the metallic region [Fig. 4(b)]. This means that the current

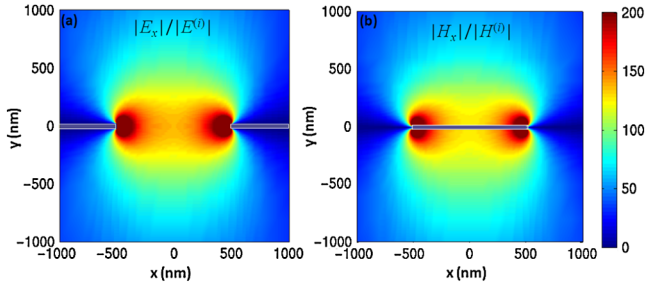

FIG. 2 (color online). Field enhancement obtained through FDTD analysis for $\lambda_0 = 3$ mm. To bring out similar field pattern, we used PEC and thin ($t = 40$ nm) metal structure. Width (w) for both structures is 1 μm. (a) E_x field enhancement at gap. (b) H_x field enhancement at wire.

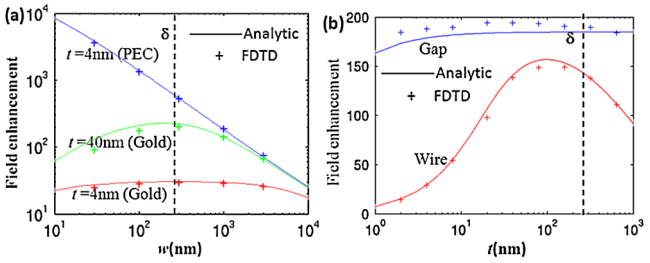

FIG. 3 (color online). (a) Magnetic field (H) enhancement for the nanowire plotted as a function of width: both analytical (lines) and FDTD analysis (+). (b) Field enhancement plotted as a function of t for nanowire (H) and nanogap (E, $\delta =$ 248 nm, $w = 1$ μm).

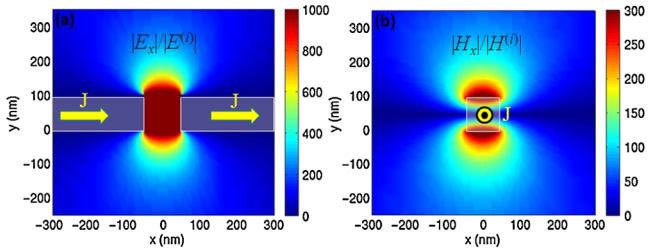

FIG. 4 (color online). Zoomed-in image of field enhancement obtained through FDTD analysis (gold, $t = 100$ nm, $w = 100$ nm). The arrows represent the current flow (J) in the metal for (a) nanogap and (b) nanowire.

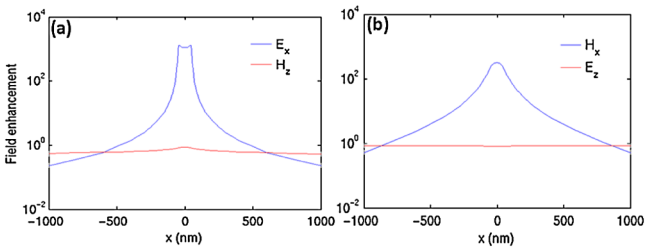

FIG. 5 (color online). Spatial distribution of the field enhancements at the exit side ($y = 100$ nm) obtained from FDTD for the same structures and material parameters as in Fig. 4. (a) nanogap and (b) nanowire.

flow is distributed within the metallic nanowire and hence, the resistance of the sub-skin-depth nanowire scales inversely with area [19] causing a saturation in the magnetic field enhancement. On the other hand for the case of nanogap, the field driven electric charges accumulate within the scale of the sub-nm Thomas-Fermi length at the gap surface [Fig. 4(a)], irrespective of the conductivity. Because of this charge accumulation on the ''surface,'' the effective width of the gap becomes independent of material conductivity as long as the gap width is considerably larger than sub-nm Thomas-Fermi length scales. Hence, in contrast to the nanowire, there is no conductivity dependent variation in the achieved electric field enhancement. To add, Fig. 5 shows the spatial distribution of the field enhancement at the exit ($y = 100$ nm) obtained from FDTD analysis for the nanogap and nanowire with same dimensions and material parameters as in Fig. 4.

To summarize, metallic nanowire structures (Babinet complementary structures for nanogaps) have been proposed and analyzed to achieve extraordinary magnetic field enhancement. Enhancement of the THz magnetic field by a factor of 300 (in terms of intensity, corresponds to a factor of 90 000) is obtained from the proposed nanowire. Analytic formulas derived incorporating thickness-normalized surface impedance concept shows that the achievable magnetic field enhancement in sub-skin-depth nanowires, though huge, cannot be as much as the electric field enhancement achieved in nanogaps. Orders of difference in the field enhancement were observed between nanogap and nanowire. More specifically, it was observed that when the cross sectional area of the nanowire becomes smaller than the square of skin depth of the material, there was a saturation in the achieved magnetic field enhancement. Our study provides detailed insights into the underlying physical phenomena that cause the deviations in classical Babinet's principle. We also believe that our rigorous theory will work as valuable guidelines for designing efficient sub-skin-depth metallic components such as the nanowire and nanoresonator, suitable for future applications in magnetic sensors and magnetic nonlinearity based devices.

This work was supported by the Korea Foundation for International Cooperation of Science & Technology (Global Research Laboratory project, K20815000003), and Korea Science and Engineering Foundation (KOSEF) grant funded by the Korea government (MEST) (R11-2008-095-01000-0).

*To whom correspondence should be addressed.
nkpark@snu.ac.kr

[1] T. W. Ebbesen *et al.*, Nature (London) **391**, 667 (1998).
[2] J. B. Pendry, L. Martín-Moreno, and F. J. García-Vidal, Science **305**, 847 (2004).
[3] W. L. Barnes, A. Dereux, and T. W. Ebbesen, Nature (London) **424**, 824 (2003).
[4] T. Matsui *et al.*, Nature (London) **446**, 517 (2007).
[5] J. W. Lee *et al.*, Phys. Rev. Lett. **99**, 137401 (2007).
[6] F. J. García de Abajo, R. Gómez-Medina, and J. J. Sáenz, Phys. Rev. E **72**, 016608 (2005).
[7] F. J. García-Vidal *et al.*, Phys. Rev. Lett. **95**, 103901 (2005).
[8] Y. Takakura, Phys. Rev. Lett. **86**, 5601 (2001).
[9] F. Yang and J. R. Sambles, Phys. Rev. Lett. **89**, 063901 (2002).
[10] H. Liu and P. Lalanne, Nature (London) **452**, 728 (2008).
[11] M. A. Seo *et al.*, Nat. Photon. **3**, 152 (2009).
[12] I. V. Shadrivov *et al.*, Opt. Express **16**, 20266 (2008).
[13] M. Born and E. Wolf, *Principles of Optics* (Pergamon, Oxford, 1964).
[14] C. Rockstuhl *et al.*, Opt. Express **16**, 2080 (2008).
[15] C. Xiang *et al.*, ACS Nano **2**, 1939 (2008).
[16] T. Senior, IEEE Trans. Antennas Propag. **25**, 417 (1977).
[17] E. Kreysziq, *Advanced Engineering Mathematics* (Wiley, Singapore, 1999).
[18] H. K. Chaurasia and W. A. G. Voss, IEEE Trans. Microwave Theory Tech. **21**, 51 (1973).
[19] M. D. Harpen, Phys. Med. Biol. **33**, 329 (1988).